# TRANSMISSION ELECTRON MICROSCOPIC STUDY OF COEXISTING PYROPHYLLITE AND MUSCOVITE: DIRECT EVIDENCE FOR THE METASTABILITY OF ILLITE[1]
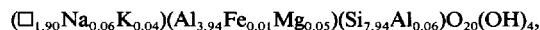
WEI-TEH JIANG, ERIC J. ESSENE, AND DONALD R. PEACOR

Department of Geological Sciences, The University of Michigan
Ann Arbor, Michigan 48109

**Abstract**—Transmission electron microscopy has been used to characterize coexisting pyrophyllite and muscovite in low-grade metamorphosed pelites from Witwatersrand and northeastern Pennsylvania. The Witwatersrand sample consisted largely of porphyroblasts of interlayered muscovite and pyrophyllite in a fine-grained matrix of the same phases. In both textures, muscovite and pyrophyllite occurred as interlayered packets (with apparently coherent interfaces) from about 300 Å to a few micrometers in thickness, with no mixed layering. Their compositions were determined with a scanning transmission electron microscope to be
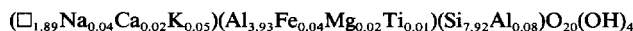
$$(\square_{0.11}K_{1.72}Na_{0.17})(Al_{3.91}Fe_{0.03}Mg_{0.05}Ti_{0.01})(Si_{6.11}Al_{1.89})O_{20}(OH)_4$$

and

$$(\square_{1.90}Na_{0.06}K_{0.04})(Al_{3.94}Fe_{0.01}Mg_{0.05})(Si_{7.94}Al_{0.06})O_{20}(OH)_4,$$

respectively.

The pyrophyllite and muscovite in the Pennsylvania shale likewise occurred only as coexisting coherent to sub-parallel packets as thin as 200 Å, with compositions of

$$(\square_{1.89}Na_{0.04}Ca_{0.02}K_{0.05})(Al_{3.93}Fe_{0.04}Mg_{0.02}Ti_{0.01})(Si_{7.92}Al_{0.08})O_{20}(OH)_4$$

and

$$(Na_{0.04}Ca_{0.02}K_{2.03})(Al_{3.54}Fe_{0.24}Mg_{0.16}Ti_{0.06})(Si_{6.09}Al_{1.91})O_{20}(OH)_4.$$

The textures of both samples were consistent with an equilibrium relationship between pyrophyllite and muscovite. The Pennsylvania sample also contained $NH_4$-rich illite, kaolinite, and an illite-like phase having intermediate Na/K, which collectively imply non-equilibrated low-grade conditions.

The compositions of these coexisting pyrophyllite and muscovite define a solvus with steep limbs and extremely limited solid solution. Illite is a white mica, intermediate in composition between pyrophyllite and muscovite, formed at much lower temperatures than muscovite. These relations show that illite is metastable relative to pyrophyllite + muscovite in all of its diagenetic and low-grade metamorphic occurrences. This further implies that illite precursor phases, such as smectite, are also metastable. The prograde reactions involving smectite, illite, and muscovite are therefore inferred to represent Ostwald-step-rule-like advances through a series of metastable phases toward the equilibrium states attained in the greenschist facies. "Illite crystallinity" can therefore be a measure of reaction progress, for which temperature is only one of several determining factors.

**Key Words**—Analytical electron microscopy, Illite, Muscovite, Pyrophyllite, Solid solution, Thermodynamic stability, Transmission electron microscopy.

## INTRODUCTION

Whether or not common clay minerals in soils and shallow sediments are thermodynamically stable is a controversial question. The term "thermodynamically stable" is used here in a strict sense: if clay minerals are thermodynamically stable, they are therefore phases in a system for which the total free energy is at a minimum for the given bulk composition, pressure, and temperature.

Most clay mineralogists have long accepted implicitly or explicitly that clays are indeed stable phases.

This view is in part suggested by observations that a given clay mineral, such as illite, has formed repeatedly in the same environment from the same and, in some occurrences, diverse starting materials. Burst (1969) and Hower *et al.* (1976) observed that smectite transforms to illite in a regular, predictable way during diagenesis of Tertiary sediments in the Gulf Coast. Hower *et al.* (1976) concluded that the transformation proceeds over a predictable temperature range and that it progresses through a series of mixed-layer phases. Likewise, illite has been observed to change with increasing grade of diagenesis/metamorphism toward muscovite, with muscovite being a stable, dioctahedral white mica under greenschist facies conditions (e.g., Hunziker *et al.*, 1986). The progressive change of illite as measured

225

by "illite crystallinity index" (e.g., Weaver, 1960; Kubler, 1964; Frey *et al.,* 1980; Kisch, 1987) is used widely as an indicator of grade for diagenesis through anchizonal conditions (i.e., for temperatures less than that of the greenschist facies). Indeed, the progressive transitions from smectite to illite to muscovite with increasing grade have been documented in many studies (for reviews, see Dunoyer de Segonzac, 1970; Kisch, 1983; Środoń and Eberl, 1984). Insofar as such relations imply equilibrium, they have been graphically represented in phase-diagram-like figures (e.g., Velde, 1969; Garrels, 1984). Such relations do not prove, however, that given phases are in a state of equilibrium; such relations are only a necessary, but most certainly not a sufficient condition for equilibrium.

The opposing view that clay minerals are metastable has been championed by Lippmann (1981, 1982) and by Essene (1982, 1989). Lippmann noted that the broad solid-solution ranges displayed by clay minerals that formed at low temperatures are at variance with the narrower ranges implied by higher temperature systems; that is, natural systems under greenschist facies and higher-temperature metamorphic conditions generally display equilibrium relations, which are verified by reversed reactions involving synthetic phases. Unless unusual conditions exist, as in the nicotine-water and di-n-propylamine-water systems (Prigogine and Defay, 1954), characteristic of a closed miscibility gap and a lower critical point, respectively, solid solution ranges of silicates should become narrower with decreasing temperature, in contrast to the observed relations for most clay minerals. In particular, Lippmann pointed out that the pyrophyllite-muscovite system is marked by a solvus having an upper critical point at higher temperatures, but that illite and (to a first approximation) smectite have intermediate compositions, commonly formed at lower temperatures than that of the upper critical point. Those phases therefore must be metastable relative to pyrophyllite + muscovite ($\pm$quartz, $H_2O$). Lippmann (1982) summarized his discussion with the generalization "if silicates would readily equilibrate at ordinary temperature, neither soils nor clays would exist and the earth would be covered by a shell of barren rocks to be classified near the greenschist facies."

The general discussions of Lippmann (1981, 1982) with respect to the significance of the solid solution limits of clay minerals vis-a-vis the limits for equivalent 2:1 phyllosilicates occurring at higher temperatures are compelling, but not absolute proof of the metastability of 2:1 clay minerals at low temperatures. In particular, well-defined data on compositions of coexisting phyllosilicates in specific natural systems are lacking. To obtain such data, two samples have been studied for which the estimated peak metamorphic temperatures are as low as possible and which contain coexisting pyrophyllite and muscovite, in order to define the stability relations between these phases. A key element of this study was the direct characterization of the samples by transmission electron microscopy (TEM) to specify structure down to the level of individual layers. Compositions of coexisting pyrophyllite and muscovite were also determined using analytical electron microscope (AEM) techniques for domains that had been characterized by structure.

## SPECIMENS AND EXPERIMENTAL TECHNIQUES

Two samples containing coexisting pyrophyllite and muscovite were studied. One was a schistose specimen from the upper part of the Witwatersrand Supergroup, Republic of South Africa. According to Phillips (1987), these rocks had been subjected to greenschist facies metamorphism and came to equilibrium at 300°–400°C and 1–2 kbars. The pelitic rocks in this region have unusual bulk compositions, being dominated by Al, Si, and K, presumably due to having been leached prior to metamorphism. They are poor in Na, Ca, and Si relative to common pelites, which otherwise would have given rise to assemblages containing quartz and feldspars.

The second specimen was studied by Juster *et al.* (1987) as part of a general investigation of prograde changes from mudstones to slates from west to east across Pennsylvania. The sample described herein was obtained from northeast Pennsylvania; Juster and Brown (1984) and Juster *et al.* (1987) inferred that it had been subjected to temperatures of 200°–275°C on the basis of observed mineral assemblages and coal rank. The range of illite crystallinity indices (0.3–0.4° $\Delta 2\theta$) suggests that conditions were anchizonal. An increase in the proportions of pyrophyllite and $NH_4$-bearing illite and a decrease in the amount of kaolinite was observed with increase in grade. Juster *et al.* (1987) identified $NH_4$-bearing illite, paragonite, pyrophyllite, chlorite, and kaolinite as the principal phyllosilicates in the rock described herein.

Powder X-ray diffractometer (XRD) patterns of bulk material were obtained first to verify that the overall mineralogy was consistent with the original descriptions. Thin sections were then prepared using "sticky wax" as the adhesive material in order to permit separation of limited areas for TEM study. The thin sections were then studied by optical and scanning electron microscopy (SEM). The SEM study involved backscattered electron (BSE) imaging combined with X-ray energy-dispersive-spectrometer analysis (EDX) using a Kevex Quantum system.

Electron microprobe analyses (EMPA) were obtained using the University of Michigan CAMECA microprobe. The EMPA analyses were made at 10 kV and 0.005 $\mu$A to minimize beam scatter and volatility of K. Volatilization checks showed that even under these conditions significant K was lost after 15 s; anal-
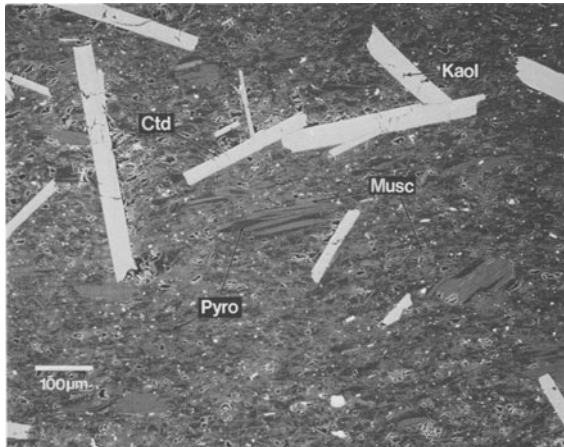
Figure 1. Back-scattered electron image of a polished thin section of the Witwatersrand sample. Large chloritoid crystals and coarse-grained porphyroblasts consisting of stacks of pyrophyllite and muscovite packets are surrounded by a matrix of fine-grained, interlayered pyrophyllite and muscovite.
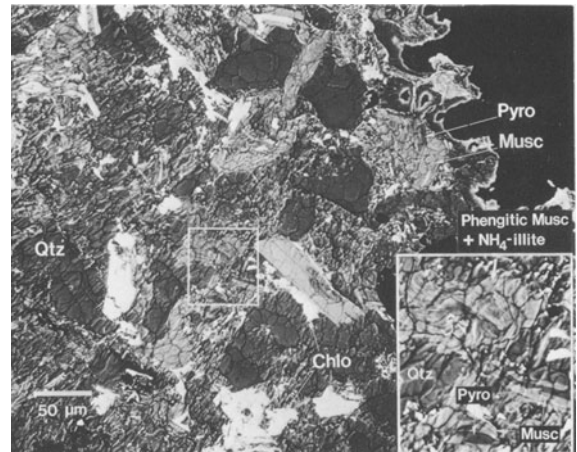


Figure 2. Back-scattered electron image of an ion-milled transmission-electron-microscopy specimen of the Pennsylvania shale. Large anhedral, detrital grains (principally quartz, feldspar, and white micas) are surrounded by a matrix composed principally of authigenic chlorite and white micas.

yses were conducted for K as the first element using 10-s counting times. The standards used were fluor-topaz for F, Tiburon albite for Na and Si, synthetic enstatite for Mg, andalusite for Al, Gotthard adularia for K, ANU wollastonite for Ca, synthetic geikielite for Ti, Broken Hill rhodonite for Mn, and synthetic ferrosilite for Fe. Initial BSE scans were used to identify areas that appeared to be single phase at the micrometer level, to minimize overlap of pyrophyllite and muscovite.

Selected areas of the thin sections were removed and ion-milled for transmission electron microscope (TEM) examination with JEOL 2000 FX and Philips CM-12 STEM instruments. The 2000 FX STEM was fitted with high- and low-angle Tracor Northern detectors, and the CM-12 STEM had a Kevex Quantum detector. Lattice-fringe images were generally obtained only using $00l$ reflections to an approximate limit of 3.3 Å, and underfocus conditions corresponding to maximum contrast. Chemical analyses were obtained in the STEM mode for areas that were first characterized by electron diffraction and lattice-fringe imaging to determine that they corresponded to single phases. Analyses were carried out using rasters as large as 1000 Å square. For K and Na analyses, raster areas and count rates for unknowns were made as nearly equal as possible to analytical conditions of the standard samples in order to minimize the differences in effects of diffusion (van der Pluijm *et al.,* 1988). Muscovite was used as a standard for Al and K, albite for Na, sphene for Ca and Ti, and chlorite for Mg and Fe. All peak intensities were calculated relative to that of Si, as a basis for normalization.

## RESULTS

### *XRD observations*

XRD patterns of the Witwatersrand sample (bulk, unseparated samples) showed the presence only of muscovite, pyrophyllite, and chloritoid, whereas patterns of the Pennsylvania pelite showed quartz, chlorite, illite, paragonite, and pyrophyllite as major phases. The d(001) value of 10.16 Å for illite is consistent with the data of Juster *et al.* (1987), who showed that this phase is an $NH_4$-bearing illite. Because of peak overlaps, however, the presence of some kaolinite, ordinary illite, and muscovite could not be ruled out.

### *SEM data*

Figure 1 is a BSE image of the Witwatersrand sample. All phases were characterized using a combination of qualitative EDX and observations of textures, consistent with optical and XRD data. The large chloritoid crystals were found to be homogeneous to the highest levels of BSE resolution, with the exception of small local areas altered to kaolinite that have the appearance of cracks in locally deformed chloritoid; the latter appeared to be a late-stage alteration product of chloritoid that occurred after synmetamorphic deformation. The texture was dominated by a fine-grained matrix of muscovite-pyrophyllite grains, with contrast differences reflecting interlayering in all grains down to a scale as low as submicrometers, and beyond the resolution of EMPA analytical techniques. Coarser grained porphyroblasts having diameters of about 100 μm in diameter were also present and consisted of interlayered packets of pyrophyllite and muscovite as thick as sev-
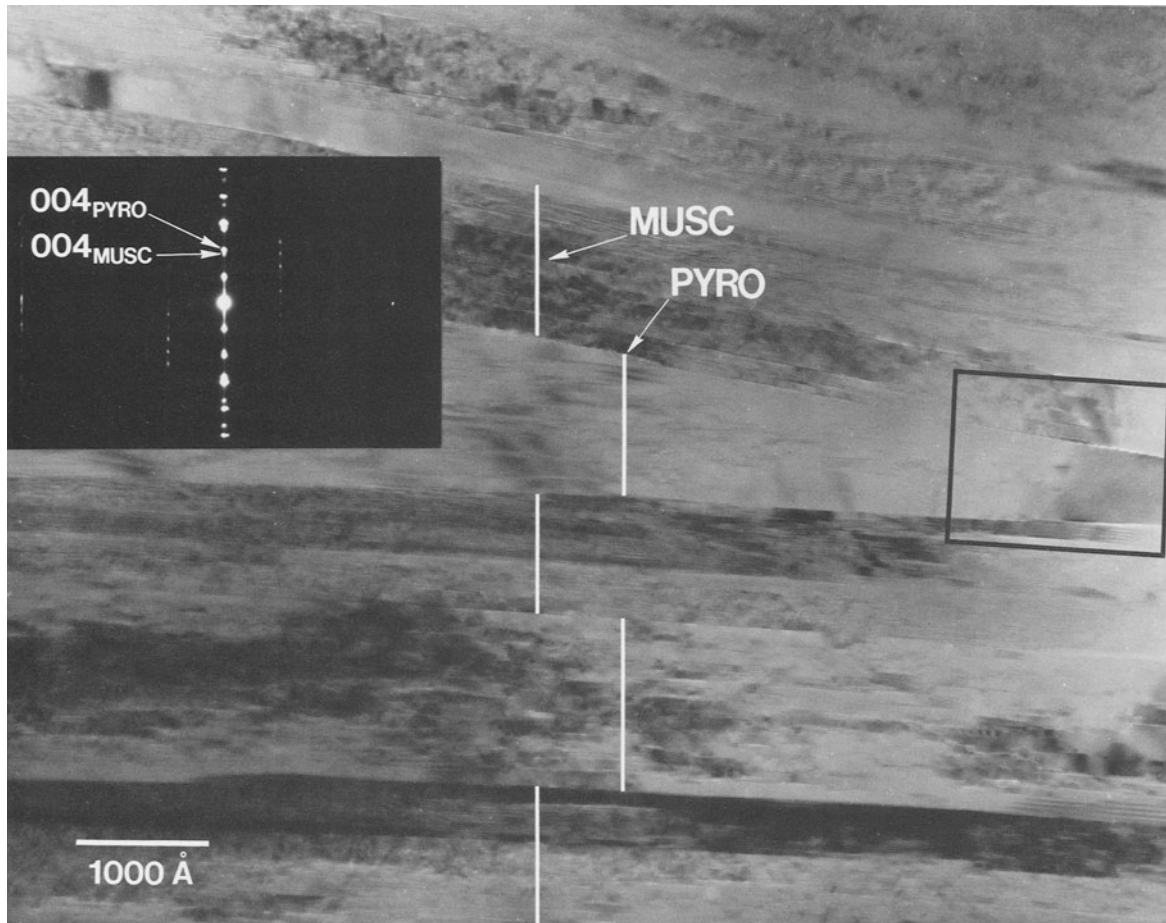
Figure 3. Low-resolution transmission-electron-microscopic image of the Witwatersrand sample showing separate packets of muscovite and pyrophyllite. Inset electron diffraction pattern shows that 001 layers of each phase are parallel.

eral tens of micrometers. Retrograde textural features were not found.

Figure 2 is a BSE image of the Pennsylvanian shale. This image was obtained using the ion-milled surface of a specimen prepared for STEM analyses in order to optimize surface polish, which ordinarily is imperfect due to the differential hardness of mineral grains. The image is dominated by large, irregular grains of quartz, feldspar, muscovite, and pyrophyllite, all of which are assumed to be detrital in origin. They are surrounded by a finer grained array consisting principally of chlorite and micaceous phases, which are inferred to be largely authigenic in origin. The EDX analyses suggest a wide range of solid solution, including muscovite, illite, pyrophyllite, and material having an Al:Si ratio consistent with illite, but having a wide range of K:Na ratios (perhaps paragonite-muscovite solid solutions). Fine-grained pyrophyllite, however, occurred as packets interlayered only with a micaceous phase that gave chemical data consistent with phengitic muscovite; it

was not found coexisting with kaolinite, illite, or illitic material having a high Na content.

*TEM data*

The TEM data for the Witwatersrand sample were obtained for both the fine-grained groundmass and for the larger porphyroblasts. Figure 3 is a typical low-resolution TEM image of both kinds of intergrowths. Packets of muscovite and pyrophyllite from a few hundred to several thousand Ångstroms in thickness alternate to form extended stacks. The inset electron diffraction pattern shows that c* of all packets is parallel, as required for coherent intergrowths, with sharp diffraction maxima and a lack of diffuseness suggesting a lack of local interlaminations of one phase in the other. Qualitative EDX analyses confirmed that packets had compositions approaching the end-members. Figure 4 is a higher resolution equivalent of a part of the image shown in Figure 3 and shows 001 lattice fringes. This area illustrates the low-angle grain bound-
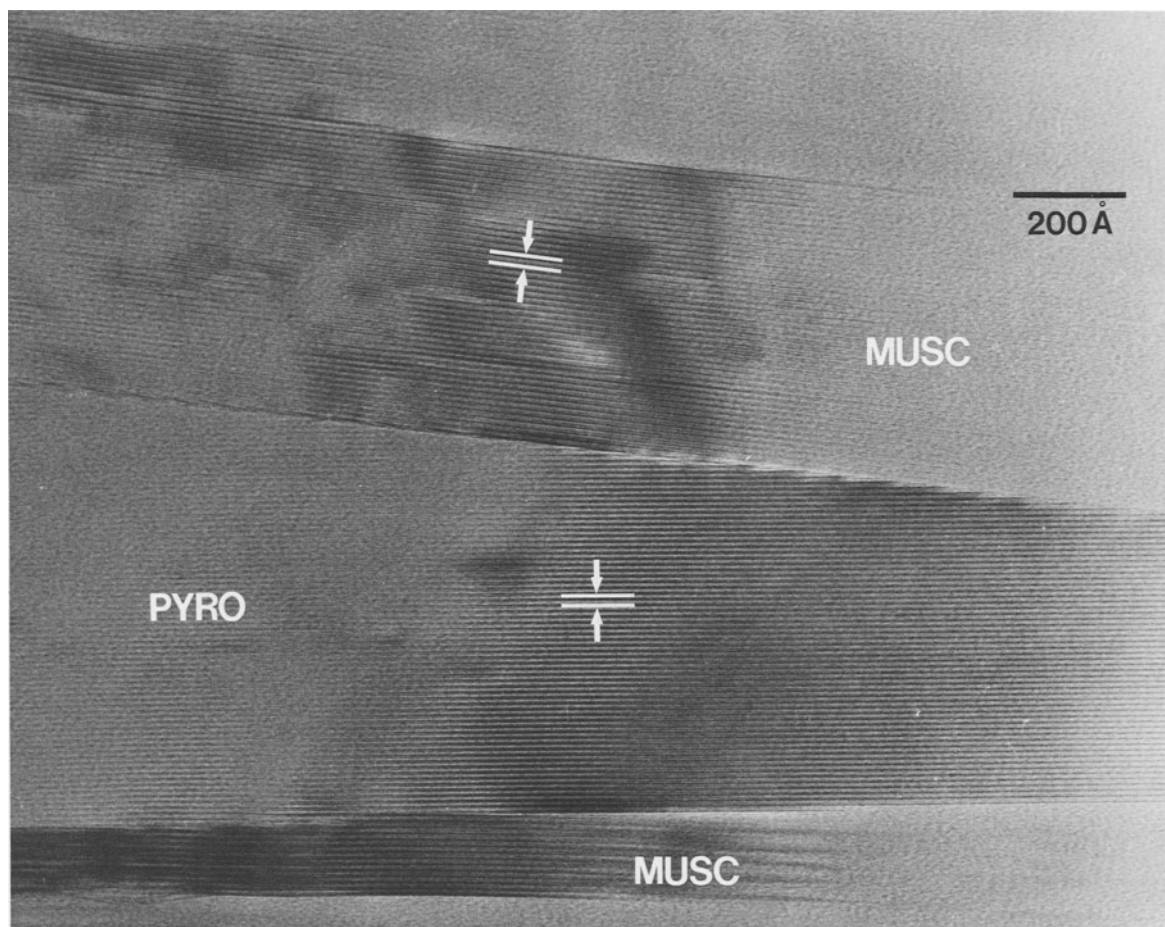
Figure 4.   High-resolution lattice fringe image that is an enlargement of the area shown in box in Figure 3. Packet of muscovite layers intersects a packet consisting only of pyrophyllite layers at a small-angle grain boundary.

ary at which pyrophyllite fringes periodically terminate against muscovite fringes. Although this intermediate scale image does not illustrate atomic-level features, the layer terminations clearly must be sites that were prime candidates for diffusion pathways for water and/or cations. The fringes in the lower packet of muscovite show two-layer periodic contrast; wherever crystals were sufficiently oriented to give rise to polytype definition, muscovite was found to be a two-layer polytype. Pyrophyllite was also invariably found to be a two-layer polytype. The lower muscovite-pyrophyllite interface in the micrograph also is largely incoherent, with fringe terminations. One fringe, however, extends continuously across the interface, giving the appearance of a continuous TOT layer. The muscovite and pyrophyllite fringes have characteristic spacings that are different enough to allow direct identification. In no particles in which measurements have been made, were muscovite layers found within pyrophyllite packets and *vice versa*, verifying the XRD and qualitative EDX data.

All of these data collectively suggest an assemblage of homogeneous phases in chemical equilibrium.

Figure 5 is a low-resolution TEM image of a pyrophyllite-muscovite intergrowth in Pennsylvanian shale. The individual packets have thicknesses ranging from a few hundred Ångstroms to more than one micrometer, with an especially large muscovite packet being imaged. The inset electron diffraction pattern shows that the muscovite and pyrophyllite packets are not parallel. Indexing of reflections was based on the two-layer polytype of muscovite and the one-layer polytype of pyrophyllite, inasmuch as these were inevitably identified if crystals were oriented properly to yield non-00*l* reflections.

Figure 6 is a higher resolution lattice-fringe image of a portion of Figure 5. Units 20 layers in thickness in adjoining muscovite and pyrophyllite have been highlighted to demonstrate the large difference in spacings that leads to the identification of individual layers. Pyrophyllite layers were not found in muscovite and
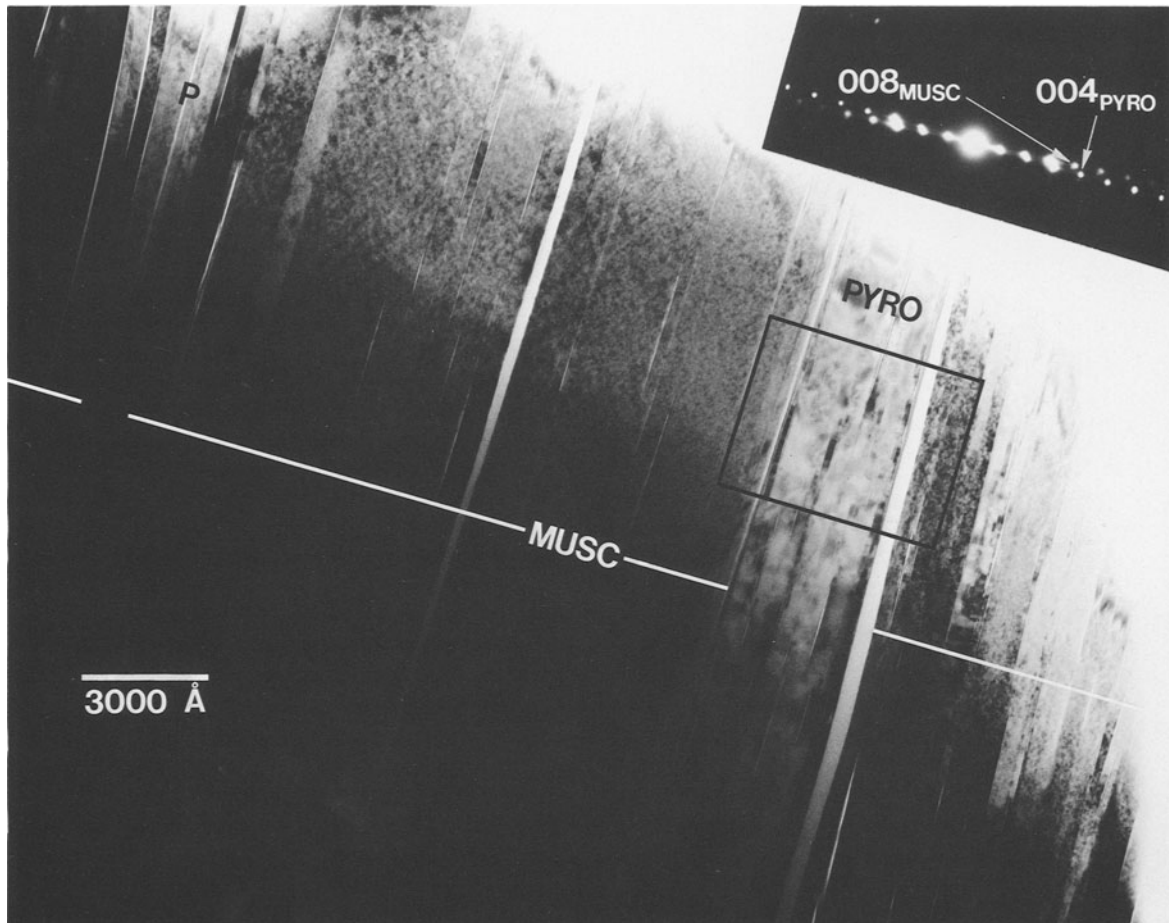
Figure 5. Low-resolution transmission-electron-microscopic image of the Pennsylvania shale showing alternating, parallel to sub-parallel packets of pyrophyllite and muscovite.

*vice versa.* Qualitative EDX analyses confirmed that compositions of packets approached end-member compositions.

Packets of layers of a third dioctahedral phyllosilicate were dominant in the matrix of the Pennsylvania sample. This phase was found to occupy the space between larger, detrital grains. A high-resolution image showing lattice fringes is shown in Figure 7. This phase is interpreted as illite, because qualitative EDX analyses consistently showed Al and K peaks that were much smaller than those for muscovite (relative to Si) and the electron diffraction pattern was that of a two-layer mica polytype. The electron diffraction pattern also showed some streaking parallel to c* as a function of interstratification of layers of variable chemistry and structure. Quantitative EDX analyses (see below) confirmed that this phase was illite and implied that it was the ammonium illite identified by Juster *et al.* (1987). All of these factors suggest that the illite was an authigenic reaction product of detrital clays, such as smectite.

A fourth dioctahedral phase having a texture akin to the illite was noted in the matrix. It had a highly variable Na:K ratio, but a composition consistent with illite having a high proportion of Na. The electron diffraction pattern was that of a 10-Å phyllosilicate. These data imply that this material was an authigenic, metastable phase containing Na and K disordered within individual layers or having Na- and K-rich layers randomly interleaved. Such a phase is probably a precursor of Na- and K-rich end members (Ahn *et al.*, 1985).

Kaolinite was rarely observed as packets of layers a few hundred Ångstroms in thickness, parallel or sub-parallel to adjacent muscovite and pyrophyllite layers in the fine-grained matrix of the Witwatersrand sample. This is a non-equilibrium assemblage and is inferred to occur either because the kaolinite, which is generally a precursor to pyrophyllite, was locally preserved or because some pyrophyllite was subjected to post-metamorphic alteration. The latter explanation is probable, as kaolinite also occurred as random aggre-

Table 1.  Chemical composition of pyrophyllite in Witwatersrand pelite.[1]

| | CP1[2] | CP2 | CP3 | CP4 | CP5 | CP6 | CP7 | FP | MEAN[3] | GNP[4] |
|---|---|---|---|---|---|---|---|---|---|---|
| $SiO_2$ | 66.33 | 66.45 | 67.21 | 65.48 | 65.75 | 66.43 | 64.45 | 66.55 | 66.38 (1.22)[5] | 66.20 |
| $Al_2O_3$ | 28.48 | 28.51 | 28.48 | 28.28 | 29.04 | 28.66 | 28.89 | 28.39 | 28.48 (0.28) | 28.19 |
| $TiO_2$ | n.d.[6] | n.d. | 0.05 | <0.02 | n.d. | 0.04 | n.d. | n.d. | 0.02 (0.04) | n.r.[6] |
| FeO | 0.22 | 0.13 | 0.09 | <0.09 | n.d. | n.d. | <0.09 | 0.20 | 0.09 (0.18) | 0.29 |
| MgO | 0.03 | 0.03 | 0.03 | 0.03 | 0.02 | 0.04 | 0.01 | <0.01 | 0.03 (0.01) | n.r. |
| MnO | 0.02 | 0.01 | n.d. | n.d. | 0.01 | n.d. | n.d. | n.d. | 0.01 (0.02) | n.r. |
| CaO | 0.08 | 0.10 | 0.07 | 0.10 | 0.07 | 0.06 | 0.07 | 0.09 | 0.08 (0.04) | n.r. |
| $Na_2O$ | 0.06 | 0.03 | 0.04 | 0.02 | 0.13 | 0.04 | 0.07 | 0.08 | 0.04 (0.02) | 0.25 |
| $K_2O$ | 0.08 | 0.08 | 0.06 | 0.06 | 0.54 | 0.13 | 0.51 | 0.07 | 0.08 (0.06) | 0.34 |
| $F_2$ | 0.13 | 0.06 | 0.15 | n.d. | n.d. | 0.06 | <0.06 | n.d. | 0.08 (0.12) | n.r. |
| $H_2O$[7] | 4.94 | 4.98 | 4.97 | 4.94 | 5.00 | 4.99 | 4.89 | 5.01 | 4.96 (0.06) | 4.77 |
| Total | 100.37 | 100.38 | 101.15 | 98.95 | 100.56 | 100.45 | 98.91 | 100.39 | 100.25 (1.60) | 100.00 |
| Si | 7.95 | 7.95 | 7.99 | 7.95 | 7.90 | 7.95 | 7.85 | 7.97 | 7.96 (0.04) | 7.95 |
| $Al^{IV}$ | 0.05 | 0.05 | 0.01 | 0.05 | 0.10 | 0.05 | 0.15 | 0.03 | 0.04 (0.04) | 0.05 |
| $Al^{VI}$ | 3.98 | 3.98 | 3.98 | 4.00 | 4.00 | 3.99 | 3.99 | 3.98 | 3.99 (0.02) | 3.99 |
| Ti | 0 | 0 | 0 | 0 | 0 | 0 | 0 | 0 | 0 | n.r. |
| Fe | 0.02 | 0.01 | 0.01 | 0 | 0 | 0 | 0.01 | 0.02 | 0.01 (0.01) | 0.01 |
| Mg | 0 | 0.01 | 0.01 | 0 | 0 | 0.01 | 0 | 0 | 0.01 (0.01) | n.r. |
| Mn | 0 | 0 | 0 | 0 | 0 | 0 | 0 | 0 | 0 | n.r. |
| Ca | 0.01 | 0.01 | 0.01 | 0.01 | 0.01 | 0.01 | 0.01 | 0.01 | 0.01 (0.00) | n.r. |
| Na | 0.01 | 0.01 | 0.01 | 0.01 | 0.03 | 0.01 | 0.02 | 0.02 | 0.01 (0.01) | 0.03 |
| K | 0.01 | 0.01 | 0.01 | 0.01 | 0.08 | 0.02 | 0.08 | 0.01 | 0.01 (0.01) | 0.02 |
| Total | 12.03 | 12.03 | 12.03 | 12.03 | 12.12 | 12.04 | 12.11 | 12.04 | 12.03 (0.01) | 12.05 |
| Positive charge | 43.97 | 43.97 | 43.97 | 43.99 | 44.05 | 43.99 | 43.96 | 44.00 | 43.99 | 43.99 |
| F | 0.05 | 0.02 | 0.06 | 0 | 0 | 0.02 | 0.02 | 0 | 0.03 (0.05) | n.r. |
| OH | 3.95 | 3.98 | 3.94 | 4.00 | 4.00 | 3.98 | 3.98 | 4.00 | 3.97 (0.05) | 4.00 |
| O | 20.00 | 20.00 | 20.00 | 20.00 | 20.00 | 20.00 | 20.00 | 20.00 | 20.00 | 20.00 |
| Negative charge | 44.00 | 44.00 | 44.00 | 44.00 | 44.00 | 44.00 | 44.00 | 44.00 | 44.00 | 44.00 |

[1] Normalization is based on total of 12 cations in tetrahedral and octahedral sites.

[2] CP and FP represent coarse-grained and fine-grained pyrophyllite crystals, respectively.

[3] Mean is average composition of coarse-grained pyrophyllite excluding CP5 and CP7 for possible interference from muscovite.

[4] Data were recalculated from Phillips' analysis (1987) and renormalized to 100 wt. %.

[5] Number in parentheses indicates two standard deviations.

[6] n.d. = not detected; n.r. = not reported.

[7] Water content was determined by assuming OH + F = 4 in the pyrophyllite structure.

gates of packets within chloritoid having a texture implying that it is likely an alteration product of chloritoid. Even though kaolinite was found in XRD patterns of the Pennsylvania shale (Juster *et al.,* 1987), we did not detect it using TEM techniques.

### Chemical analyses

Electron microprobe analyses (Tables 1 and 2) were obtained for the individual packets of pyrophyllite and muscovite in the large porphyroblasts of the Witwatersrand sample, inasmuch as packets of all other pyrophyllite and muscovite in the fine-grained matrix were too small to be resolved by this technique. Analyses of the chloritoid and kaolinite are given in Table 3 for completeness. The microprobe analyses (Tables 1 and 2) of the coexisting pyrophyllite and muscovite from Witwatersrand reveal little mutual solid solution, in good agreement with the results of Phillips (1987).

The EDX analyses were obtained using STEM techniques on packets of layers that had been found by

TEM to consist of a single phase (Table 4). The data for the Witwatersrand sample are for packets from grains in the fine-grained matrix; however, comparison of the STEM and EMPA data shows that muscovite and pyrophyllite from both matrix and porphyroblasts had nearly identical compositions. The data show that the coexisting muscovite and pyrophyllite in both samples had compositions that approach those of the ideal end-members, with only minor solid solution. Table 4 also gives an analysis of the ammonium illite. The ammonium content is only implied by the data, as such small amounts of nitrogen that are required cannot be detected by the EDS system. Juster *et al.* (1987) showed that such a phase is abundant in this sample. As it stands, our analysis is markedly deficient in interlayer cations with a resulting severe charge imbalance, as would be expected for such an ammonium (or hydronium) illite. Analytical error has been ruled out as a cause because the analyses of all other phyllosilicates, which were obtained in the same sessions, give well-balanced formulae.
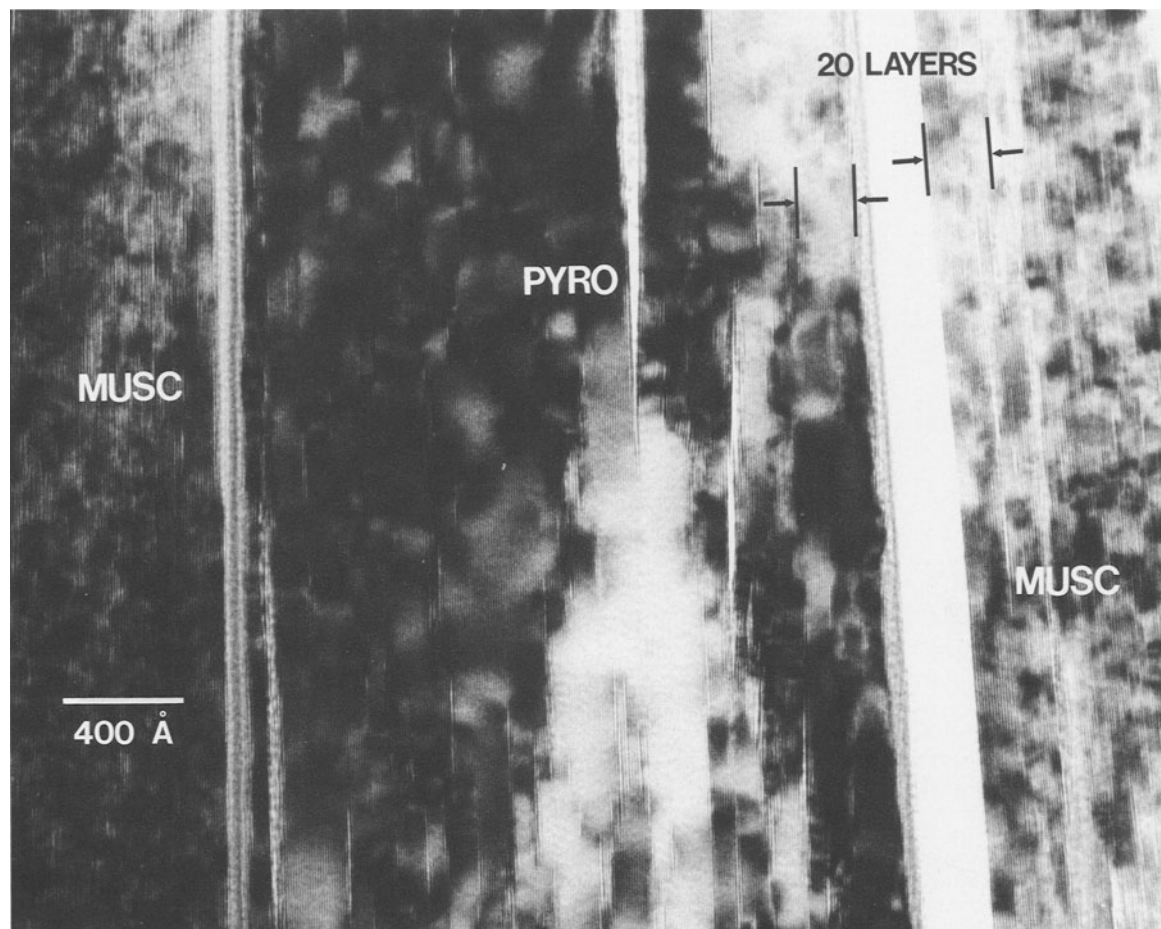
Figure 6.   High-resolution lattice-fringe image that is an enlargement of the area shown in box in Figure 5. Widths corresponding to 20 layers of both pyrophyllite and muscovite are outlined, showing that the interplanar spacings are diagnostic.

## DISCUSSION

### General relations concerning stability of clay minerals

The question of whether or not clay minerals can be stable phases is, in principle, determinable utilizing experimental data that generally fall into one of two categories: (1) direct experiments, and (2) calculation of stability relations based on thermodynamic parameters. Meaningful experiments at the low temperatures of clay mineral formation are difficult to obtain because reaction rates are too slow to permit an approach to equilibrium (Lippmann, 1981; Yau *et al.,* 1987). An even greater problem is that reversals of equilibrium states cannot in general be achieved, and it is only through such experimental reversals that equilibrium can be proven. Accurate thermodynamic parameters cannot in general be experimentally measured because clay minerals are heterogeneous materials, and resulting experimental values cannot be correlated with specific structures and chemistries (May *et al.,* 1986). The problem is exacerbated by the fact that even if thermodynamic parameters could be determined for pure end members, they can be used at best only in an approximate way with respect to calculating parameters for solid solutions because of a lack of knowledge of activity vs. composition relations.

Experimental problems at low temperatures can perhaps be minimized in aqueous dissolution experiments. May *et al.* (1986) discussed the problems attendant to such experiments in detail and provided an extensive literature survey. They concluded that "detailed examination of earlier reports of solubility-based $\Delta G_f$ determinations for aluminous 2:1 phyllosilicate clay minerals makes clear that truly reversible equilibrium solubility (in aqueous media at 25°C), and the valid derivation of $\Delta G_f$ values therefrom, have *never* been unequivocally demonstrated in experiments with these complex minerals." They noted that the problem is largely inherent in the heterogeneity of experimental clay minerals and in the substitution mechanisms, which are not precisely known for any given specimen.

Table 2. Chemical composition of muscovite in Witwatersrand pelite.[1]

| | CM1[2] | CM2 | CM3 | CM4 | CM5 | CM6 | CM7 | CM8 | FM | MEAN[3] | GNP[4] |
|---|---|---|---|---|---|---|---|---|---|---|---|
| $SiO_2$ | 46.16 | 46.60 | 46.40 | 46.09 | 47.74 | 45.98 | 47.21 | 46.29 | 47.65 | 46.25 (0.46)[5] | 47.51 |
| $Al_2O_3$ | 37.30 | 37.79 | 37.80 | 37.65 | 37.45 | 37.77 | 36.62 | 37.28 | 37.66 | 37.60 (0.48) | 36.79 |
| $TiO_2$ | 0.04 | n.d.[6] | 0.05 | 0.06 | 0.06 | <0.03 | 0.04 | n.d. | <0.03 | 0.03 (0.06) | n.r.[6] |
| $FeO$ | 0.76 | 0.14 | 0.12 | 0.26 | 0.29 | 0.23 | n.d. | 0.21 | 0.18 | 0.29 (0.48) | 0.59 |
| $MgO$ | 0.25 | 0.15 | 0.11 | 0.19 | 0.10 | 0.13 | 0.11 | 0.13 | 0.13 | 0.16 (0.10) | n.r. |
| $MnO$ | 0.10 | n.d. | n.d. | 0.06 | n.d. | 0.05 | n.d. | 0.10 | n.d. | 0.04 (0.08) | n.r. |
| $CaO$ | 0.04 | 0.13 | <0.04 | n.d. | 0.04 | 0.05 | 0.05 | <0.04 | 0.08 | 0.05 (0.08) | n.r. |
| $Na_2O$ | 0.78 | 0.90 | 0.76 | 0.85 | 1.00 | 0.83 | 0.81 | 0.84 | 1.06 | 0.83 (0.10) | 1.03 |
| $K_2O$ | 9.71 | 9.57 | 9.96 | 9.82 | 9.14 | 10.05 | 9.31 | 10.10 | 9.00 | 9.87 (0.42) | 9.29 |
| $F_2$ | n.d. | n.d. | 0.13 | <0.05 | n.d. | n.d. | 0.15 | n.d. | n.d. | <0.05 (0.10) | n.r. |
| $H_2O$[7] | 4.54 | 4.57 | 4.50 | 4.52 | 4.61 | 4.54 | 4.46 | 4.53 | 4.62 | 4.53 (0.04) | 4.79 |
| Total | 99.68 | 99.85 | 99.86 | 99.54 | 100.43 | 99.64 | 98.86 | 99.39 | 100.40 | 99.67 (0.38) | 100.00 |
| Si | 6.07 | 6.11 | 6.10 | 6.07 | 6.20 | 6.06 | 6.24 | 6.13 | 6.18 | 6.09 (0.06) | 6.24 |
| $Al^{IV}$ | 1.93 | 1.89 | 1.90 | 1.93 | 1.80 | 1.94 | 1.76 | 1.87 | 1.82 | 1.91 (0.06) | 1.76 |
| $Al^{VI}$ | 3.86 | 3.96 | 3.97 | 3.91 | 3.94 | 3.93 | 3.94 | 3.95 | 3.95 | 3.93 (0.08) | 3.94 |
| Ti | 0 | 0 | 0 | 0.01 | 0.01 | 0 | 0 | 0 | 0 | 0 (0.01) | n.r. |
| Fe | 0.08 | 0.01 | 0.01 | 0.03 | 0.03 | 0.03 | 0.03 | 0.02 | 0.02 | 0.03 (0.05) | 0.06 |
| Mg | 0.05 | 0.03 | 0.02 | 0.04 | 0.02 | 0.03 | 0.03 | 0.03 | 0.03 | 0.03 (0.02) | n.r. |
| Mn | 0.01 | 0 | 0 | 0.01 | 0 | 0.01 | 0 | 0 | 0 | 0.01 (0.01) | n.r. |
| Ca | 0.01 | 0.02 | 0 | 0 | 0.01 | 0.04 | 0 | 0 | 0 | 0 (0.03) | n.r. |
| Na | 0.20 | 0.23 | 0.19 | 0.22 | 0.25 | 0.21 | 0.18 | 0.22 | 0.27 | 0.21 (0.03) | 0.26 |
| K | 1.63 | 1.60 | 1.67 | 1.65 | 1.52 | 1.69 | 1.43 | 1.71 | 1.49 | 1.66 (0.08) | 1.56 |
| Total | 13.84 | 13.85 | 13.86 | 13.87 | 13.78 | 13.93 | 13.61 | 13.93 | 13.77 | 13.88 (0.08) | 13.82 |
| Positive charge | 43.79 | 44.00 | 43.93 | 43.81 | 43.95 | 43.96 | 43.79 | 44.01 | 43.91 | 43.92 | 44.00 |
| F | 0 | 0 | 0.05 | 0.02 | 0 | 0 | 0.06 | 0 | 0 | <0.02 (0.04) | n.r. |
| OH | 4.00 | 4.00 | 3.95 | 3.98 | 4.00 | 4.00 | 3.94 | 4.00 | 4.00 | 4.00 (0.04) | 4.00 |
| O | 20.00 | 20.00 | 20.00 | 20.00 | 20.00 | 20.00 | 20.00 | 20.00 | 20.00 | 20.00 | 20.00 |
| Negative charge | 44.00 | 44.00 | 44.00 | 44.00 | 44.00 | 44.00 | 44.00 | 44.00 | 44.00 | 44.00 | 44.00 |

[1] Normalization is based on total of 12 cations in tetrahedral and octahedral sites.
[2] CM and FM represent coarse-grained and fine-grained muscovite crystals, respectively.
[3] Mean is average composition of coarse-grained muscovite excluding CM5 and CM7 for possible interference of pyrophyllite.
[4] Data were recalculated from Phillips' analysis (1987) and renormalized to 100 wt. %.
[5] Number in parentheses indicates two standard deviations.
[6] n.d. = not detected; n.r. = not reported.
[7] Water content was determined by assuming OH + F = 4 in the muscovite structure.
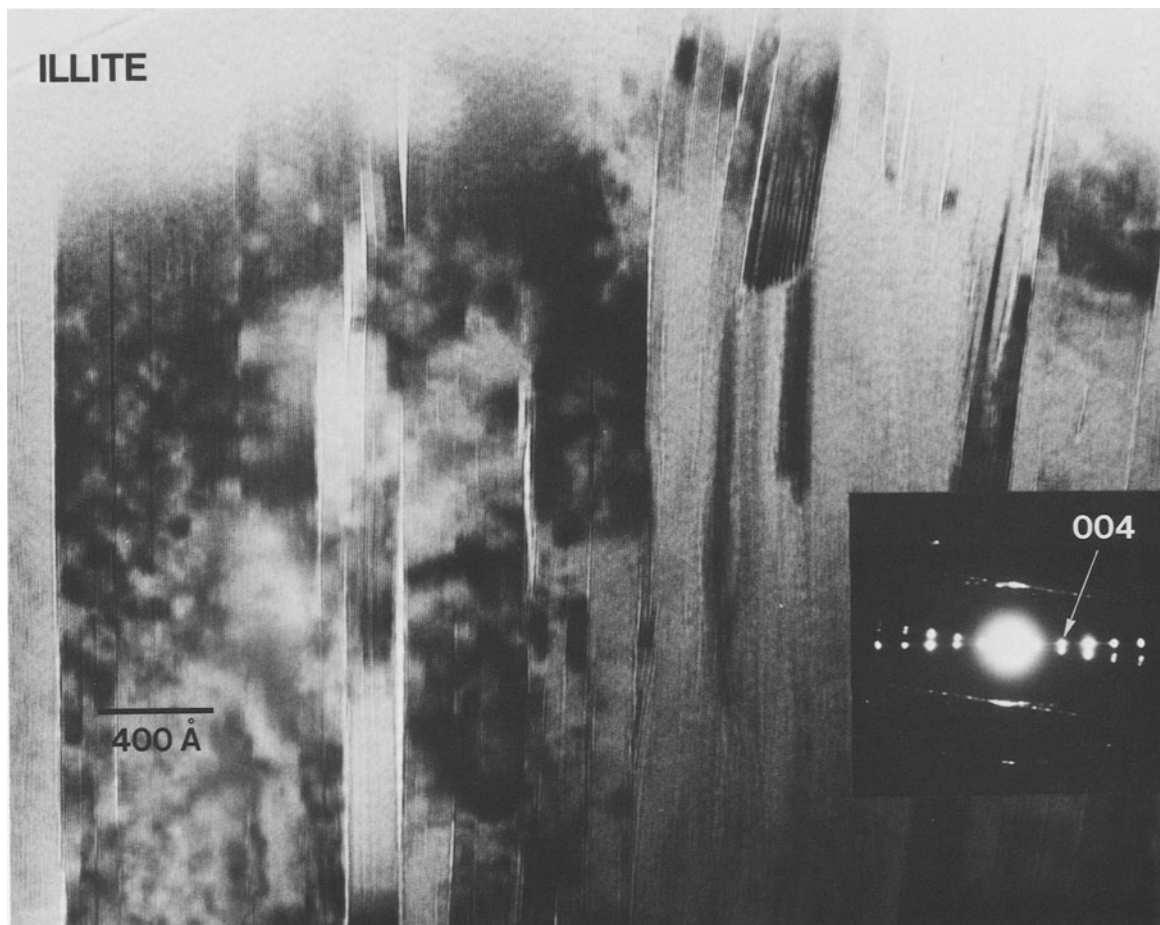
Figure 7. Lattice-fringe image of packets of ammonium illite (see text for detail).

On the other hand, Sass *et al.* (1987) used natural illite samples in solution experiments and concluded that the illite-smectite transition that occurred between 90 and 110°C acted to stabilize the assemblages illite-smectite-kaolinite and illite-smectite-microcline. They claimed to have obtained reversals of equilibria and to have compensated for compositional heterogeneity through high-resolution characterization of domains involved in reactions. We are somewhat skeptical of this claim.

It is difficult, if not impossible, to arrive at unambiguous conclusions regarding the stability of clay minerals on the basis of experimental data. A more direct way exists, however, to assess stability relations, and that is to obtain data for natural systems in which the chemical/structural/textural data imply an approach to equilibrium conditions. In general, this approach may require that observations be made for rocks that have been subjected to temperatures that are as high as possible, while still retaining the minerals that are characteristic of the low-temperature environment. Reactions in natural samples subjected to regional metamorphic conditions take place over times that are

orders of magnitude greater than those attainable in the laboratory. The samples examined in this study represent such relations.

Merino and Ransom (1982) calculated the free energies for the formation of illite solid solutions using the compositions of illites and interstitial water in sandstones by assuming that they had reached an equilibrium state. Their data show that most of the interstitial waters were undersaturated with respect to quartz and that the assumption of equilibrium with respect to illite needed further evaluation. Their electron microprobe analyses of illite, which had low totals, showed that its composition varied from nearly pyrophyllite to muscovite end members. Such heterogeneity is strongly indicative of a lack of equilibrium in the solid samples that were analyzed. Indeed, clay minerals, such as illite and smectite, are ubiquitously heterogeneous, further implying a general lack of equilibrium.

The definition of illite has been much discussed (e.g., Šrodoń and Eberl, 1984); however, most workers agreed that illite is a fine-grained "white mica" that forms in soils and sediments at low temperatures (Grim, 1968). General agreement also exists that the composition of

Table 3. Chemical compositions of chloritoid and kaolinite in Witwatersrand pelite.[1,2]

|  | CTD | GNP[3] | KAOL |
|---|---|---|---|
| $SiO_2$ | 24.06 (0.38)[4] | 26.13 | 45.94 (1.02) |
| $Al_2O_3$ | 40.92 (0.36) | 40.53 | 38.92 (0.60) |
| $Cr_2O_3$ | n.d.[5] | 0.15 | n.d. |
| $TiO_2$ | 0.04 (0.04) | n.r.[5] | 0.04 (0.04) |
| FeO | 24.73 (0.80) | 23.11 | 0.42 (0.36) |
| MgO | 1.47 (0.16) | 2.36 | 0.04 (0.06) |
| MnO | 1.02 (0.18) | 0.43 | 0.01 (0.04) |
| CaO | 0.02 (0.02) | n.r. | 0.11 (0.14) |
| $Na_2O$ | 0.01 (0.01) | n.r. | 0.04 (0.06) |
| $K_2O$ | 0.03 (0.06) | n.r. | 0.02 (0.02) |
| $H_2O$[6] | 7.20 (0.04) | 7.29 | 13.83 (0.28) |
| Total | 99.50 (0.74) | 100.00 | 99.37 (1.64) |
| Si | 2.00 (0.03) | 2.15 | 3.98 (0.03) |
| Al | 4.01 (0.50) | 3.93 | 3.98 (0.01) |
| Cr | 0 | 0.01 | 0 |
| Ti | 0 | n.r. | 0 |
| Fe | 1.72 (0.05) | 1.59 | 0.03 (0.03) |
| Mg | 0.18 (0.02) | 0.29 | 0.01 (0.01) |
| Mn | 0.07 (0.01) | 0.03 | 0 |
| Ca | 0 | n.r. | 0.01 (0.01) |
| Na | 0 | n.r. | 0.01 (0.01) |
| K | 0 | n.r. | 0 |
| Total | 8.00 | 8.00 | 8.02 (0.02) |
| Positive charge | 24.02 | 24.24 | 27.97 |
| OH | 4.00 | 4.00 | 8.00 |
| O | 10.00 | 10.00 | 10.00 |
| Negative charge | 24.00 | 24.00 | 28.00 |

[1] All analyses were averaged from compositions of several analyzed points.

[2] Normalization is based on total of 8 cations in tetrahedral and octahedral sites for both chloritoid and kaolinite.

[3] Data were recalculated from Phillips' analysis (1987) and renormalized to 100 wt. %.

[4] Number in parentheses indicates two standard deviations.

[5] n.d. = not detected; n.r. = not reported.

[6] Water contents were determined by assuming OH = 4 and 8 for chloritoid and kaolinite, respectively.

illite is such that it is derived by the substitution of Si for K + Al in muscovite; i.e., illite is deficient in K and Al and enriched in Si relative to muscovite, with the vacancies in the interlayer cation sites approaching 50% of the available sites. Illite also contains ubiqui-tous small concentrations of Fe and Mg, generally assumed to be present in octahedral sites (i.e., as a phengitic substitution). The composition of illite falls on the pyrophyllite-muscovite join, and the presence of Mg and Fe in illite may be accounted for by consid-

Table 4. Analytical electron microscopic analyses of muscovite and pyrophyllite in Witwatersrand and Pennsylvania pelites.[1,2]

|  | Witwatersrand, Republic of South Africa | | Blackridge, Pennsylvania | | |
|---|---|---|---|---|---|
|  | Muscovite | Pyrophyllite | Muscovite | Pyrophyllite | $NH_4$-illite |
| Si | 6.11 (0.10)[3] | 7.94 (0.23) | 6.09 (0.16) | 7.92 (0.16) | 6.37 (0.27) |
| $Al^{IV}$ | 1.89 (0.10) | 0.06 (0.23) | 1.91 (0.16) | 0.08 (0.16) | 1.63 (0.27) |
| $Al^{VI}$ | 3.91 (0.09) | 3.94 (0.12) | 3.54 (0.13) | 3.93 (0.15) | 3.78 (0.31) |
| Ti | 0.01 (0.02) | n.d.[4] | 0.06 (0.01) | 0.01 (0.03) | 0.01 (0.02) |
| Fe | 0.03 (0.02) | 0.01 (0.01) | 0.24 (0.05) | 0.04 (0.03) | 0.11 (0.09) |
| Mg | 0.05 (0.05) | 0.05 (0.04) | 0.16 (0.06) | 0.02 (0.02) | 0.10 (0.11) |
| Ca | n.d. | n.d. | 0.02 (0.03) | 0.02 (0.01) | 0.02 (0.03) |
| Na | 0.17 (0.11) | 0.06 (0.11) | 0.04 (0.01) | 0.04 (0.03) | 0.03 (0.04) |
| K | 1.72 (0.19) | 0.04 (0.07) | 2.03 (0.20) | 0.05 (0.03) | 0.63 (0.53) |
| Total | 13.89 (0.26) | 12.10 (0.15) | 14.09 (0.17) | 12.11 (0.02) | 12.68 (0.54) |
| Positive charge | 43.93 | 43.98 | 43.86 | 44.00 | 42.87 |

[1] All analyses were derived as an average of several scanning areas.

[2] Normalization is based on total of 12 cations in tetrahedral and octahedral sites.

[3] Number in parentheses indicates two standard deviations.
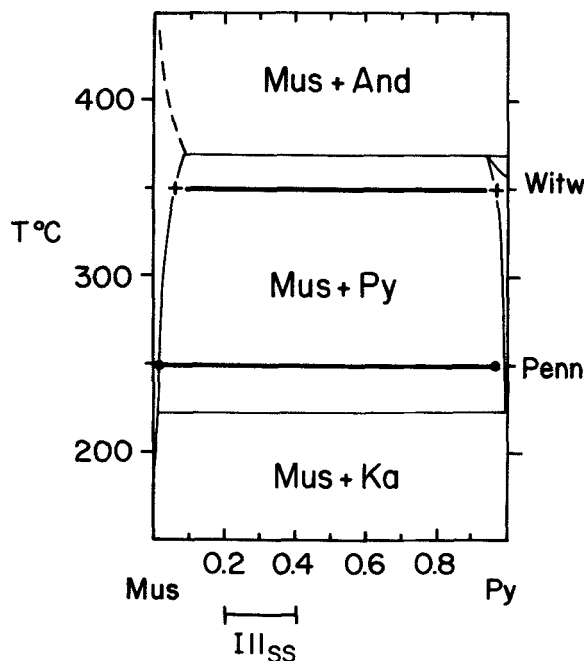
[4] n.d. = not detected.

Figure 8. Compositions of coexisting muscovite and pyrophyllite of the Witwatersrand (+) and Pennsylvania (●) samples, plotted on the muscovite-pyrophyllite binary, with estimated positions of limbs of solvus. Diagram was constructed with quartz and $H_2O$ in excess at 2 kb and shows approximate equilibrium stability fields for kaolin, pyrophyllite, and andalusite with increasing temperature.

eration of solid solution with phengite. If a stable solvus exists between muscovite and pyrophyllite under the low-temperature conditions at which illite forms, illite must be metastable relative to pyrophyllite + muscovite. This result in turn has profound consequences for theories of diagenesis, not only of illite, but for smectite and other clay minerals as well.

*Experimental data*

The present data show that dioctahedral phyllosilicates in the Witwatersrand sample are muscovite and pyrophyllite occurring as intergrown, homogeneous packets of layers. The compositions of the phases in both the fine-grained groundmass and in coarser porphyroblasts are identical within error; this implies that the mineral relations reflect equilibrium conditions that were attained at the peak of metamorphism.

The texture of the Pennsylvania shale sample is clearly that of a sediment that has been modified by diagenesis or very low grade metamorphism. The coexistence of four separate dioctahedral mica-like phases (muscovite, pyrophyllite, Na/K illite, ammonium illite) clearly is a reflection of non-equilibrium conditions. Each of the two varieties of illite-like phases was observed to be heterogeneous in composition within individual grains, a clear indication of a lack of chemical equilibrium. On the other hand, pyrophyllite and muscovite were noted only intergrown with one another, each as

homogeneous packets of layers. The compositions are identical (within error) from grain to grain and near the theoretical end members; layers are relatively defect-free, and muscovite occurs as a well-ordered two-layer polytype. All of these features are consistent with equilibrium conditions (Lee *et al.,* 1986). Baxter and Peacor (1988) showed that authigenic illite in its initial state of formation occurs in a disordered one-layer state, whereas illite/muscovite that is a subsequent dissolution-crystallization product occurs chiefly as a well-ordered two-layer polytype.

The above-described STEM/SEM relations collectively imply that the pyrophyllite and muscovite represent local equilibration in the Pennsylvania pelite under peak metamorphic conditions, such that the bulk of the phases still retain textural features and compositions that reflect incomplete reaction of authigenic phases formed at lower temperatures or detrital phases retaining predepositional compositions and structures. The proportion of kaolinite decreases and that of pyrophyllite increases with increasing grade in the sample area (Juster *et al.,* 1987), further implying that pyrophyllite is a stable phase under conditions of metamorphism.

*Metastability of illite*

The data presented above show that in the two samples studied, muscovite and pyrophyllite coexist under equilibrium conditions. In the sample from Pennsylvania, the equilibrium relations occur only on a local basis, but in the Witwatersrand sample, equilibrium relations exist throughout the sample. These relations define a solvus with steep limbs and extremely limited solid solution. Few other microprobe analyses of coexisting pyrophyllite and muscovite are available for comparison in the literature. The two analyses of muscovites coexisting with pyrophyllite from greenschist facies rocks in the northern Apennines, Italy, in Franceschelli *et al.* (1986), show ~11% vacancies in the muscovite, slightly more than in the Witwatersrand micas. Frey *et al.* (1988) described metasediments from Trinidad that contain micrometer-size interlayered pyrophyllite, paragonite, and muscovite. They estimated equilibration temperatures at 300°–350°C at pressures >2 kb. Microprobe analyses of coexisting pyrophyllite and muscovite gave $Py_{94.8}Pg_{3.9}Mg_{0.6}Mu_{0.7}$ and $Mu_{78.8}Py_{11.5}Pg_{9.3}Mg_{0.4}$, respectively, although some overlap of adjacent mica and pyrophyllite layers was likely. Franceschelli *et al.* (1989) reported the assemblage pyrophyllite-muscovite-sudoite-quartz in low-grade metamorphic rocks of the northern Apennines and estimated conditions as 330° ± 40°C and <5 kb. They found intergrown pyrophyllite-muscovite-sudoite at the 1–10-μm scale. Analyses of the muscovite gave $Mu_{74}Pg_{13}Py_{13}$ in equilibrium with nearly pure pyrophyllite. Ghent *et al.* (1989) analyzed pyrophyllite coexisting with chloritoid, calcite, ankerite, and intergrown paragonite-muscovite in slates from British Co-

lumbia. Their analysis of pyrophyllite shows $Py_{98.5}Pg_{1.2}Mu_{0.3}$. Even if these microprobe analyses represent some overlap of pyrophyllite and mica crystallites, they all indicate only very limited mutual solid solution between pyrophyllite and muscovite in low-grade metamorphic rocks. Because the composition of illite is intermediate to that of pyrophyllite and muscovite, illite cannot be thermodynamically stable at temperatures at which pyrophyllite and muscovite are stable, coexisting phases.

The effect of Mg and Fe solid solutions on the stability of illite vs. muscovite-pyrophyllite must also be considered. These elements are generally assumed to substitute as phengite-type exchanges in illite (i.e., [Mg, $Fe^{2+}$] + Si = Al + Al), as is true in muscovite. Whether these solid solutions stabilize illite solid solution over pyrophyllite + muscovite solid solution can be evaluated by consideration of pyrophyllite-phengite assemblages. Because muscovite may incorporate extensive phengite substitution at low temperatures and high pressures (e.g., Velde, 1965; Massonne and Schreyer, 1987; Bucher-Nurminen, 1987), it seems unlikely that illite would become stable as a result of this substitution. The case of $Fe^{3+}$ in illite is similar: muscovite may contain substantial octahedral $Fe^{3+}$ substituting for Al (e.g., Foster, 1956; Kanehira and Banno, 1960). Even though much of the Fe in illite may be $Fe^{3+}$ rather than $Fe^{2+}$, the similar capacity of muscovite to absorb $Fe^{3+}$ implies that this ion is unlikely to stabilize illite over muscovite + pyrophyllite. Baldelli *et al.* (1989) showed ~7% interlayer vacancies in muscovite with some celadonite-type substitution, coexisting with pyrophyllite in $Fe^{3+}$-rich rocks of the Verrucano metasediments of North Apennines, Italy. Their result implied that the substitution of celadonite component for muscovite could not result in formation of illite solid solution. Similar arguments may be advanced for other solid solutions in illite. The possible effect of hydronium ($H_3O^+$) substitution on the stability of illite and muscovite also needs evaluation.

The hydronium-mica component may be related to pyrophyllite by the reaction:

$$2(H_3O)Al_2(Si_3Al)O_{10}(OH)_2 + 6SiO_2$$
$$= 3Al_2Si_4O_{10}(OH)_2 + 2H_2O.$$
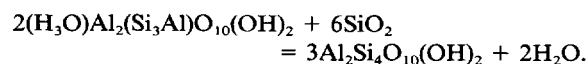
Thus, hydronium substitution should be maximized in the presence of pyrophyllite at high water pressure and low temperature. It would also be buffered internally in an illite solid solution equilibrated with quartz and water. There, the hydronium-mica component should be inversely related to the pyrophyllite component at a given P and T. This implies that the latter component is more important in illite. The substitution $H_3O^+ = K^+$ is difficult to resolve from $\square + Si = K + Al$ with electron microbeam analyses of complex illite solid solution, and direct spectral measurements are needed to evaluate the importance of hydronium substitutions in clays and micas. Whereas the form of the

pyrophyllite-muscovite miscibility gap may be modified by solid solutions in muscovite, the conclusion as to illite metastability is unlikely to be changed.

The question remains whether illite can possess a stability field at lower temperatures than those at which pyrophyllite and muscovite are separated by a wide miscibility gap (Figure 8). This scenario requires that illite has a lower entropy than muscovite + pyrophyllite. If illite has a disordered structure with extensive solid solutions of vacancies and K, its entropy is unlikely to be low. On the other hand, if illite has an ordered structure, i.e., made up of units containing 1 K (per 24 anions) alternating with units of 2 K in a highly ordered two-layer structure, as hypothesized by Šrodoń *et al.* (1986), illite could possibly be stabilized at low temperatures by a reduced entropy relative to a mechanical mixture of pyrophyllite and muscovite. No crystal structure or TEM/AEM data, however, are available to suggest that illite has such a structure; indeed, the opposite is true. Such a structure would give rise to characteristic features in electron diffraction patterns that have not been observed by any investigators. This possibility is therefore not relevant, and illite must be metastable in all of its occurrences, with pyrophyllite + muscovite being the stable equivalents. Although the limits of muscovite solid solutions appear to be larger at higher temperatures, illite has never been observed in rocks formed at higher temperatures, probably because the formation of micaceous phases is buffered by the breakdown of pyrophyllite to andalusite at high temperatures, giving rise to muscovite instead of illite (Fig. 8).

Since the pioneering studies of Burst (1959) and Hower *et al.* (1976), many investigations of diagenesis of pelitic rocks in sedimentary basins have verified that the normal sequence of clay mineral transitions, in which dioctahedral smectite is the original detrital clay, is: smectite → random mixed-layer I/S → R1 ordered I/S → R3 ordered I/S → illite (e.g., Burtner and Warner, 1986; Nadeau and Reynolds, 1981; Hoffman and Hower, 1979; Chang *et al.,* 1986). Although mixtures of the various phases may exist, or the sequence may not appear to be complete, the general form of the sequence is found almost universally. The original detrital smectite in such sequences is a terrestrial weathering product, commonly having volcanic ash as its source.

Because the sequence trends toward illite, and because illite is a metastable phase, the smectite and mixed-layer phases must likewise be metastable where they occur. If a given phase or assemblage of phases spontaneously reacts to give rise to a metastable phase (illite), then the original phases must have constituted a system with even higher free energy than that of the system containing the metastable reactant. In the absence of input of energy, chemical systems change spontaneously in directions toward the assemblage for which the free energy of the system is a minimum. For these clay mineral reactions, the assemblage must in-

clude at least smectite, illite, quartz, aqueous solution ±K-feldspar. The degree of conversion of one clay mineral to another extending over an interval of 100°C or so could only represent an equilibrium sequence if the composition of one or more of the phases (including the aqueous solution) is changing significantly over the same temperature range. An additional difficulty exists in defining phases for structures that are interlayered over scales of <1000 Å: each coherent or semicoherent package of phyllosilicates will be a thermodynamically distinct phase, but all such phases will be metastable with respect to a mechanical mixture of coarse-grained equivalent phases. In summary, the complex submicroscopic intergrowths of phyllosilicates have all the characteristics of a system that formed metastably at low temperatures at or near the surface of the Earth; furthermore, their progressive reaction to successively more stable assemblages at increasing depths and temperatures is strongly suggestive of a highly unstable system tending towards equilibrium through a series of progressively more stable intermediates. The sequence of phases observed in geological systems from smectite to I/S to illite to muscovite is a classic example of a disequilibrium chemical system driving toward a state of stable equilibrium.

If illite is a metastable phase that lies on the pyrophyllite-muscovite join, activity/composition relations and the excess free energy of mixing relations should reflect the wide solvus in the pyrophyllite-muscovite system. No direct measurements have yet been made, but several workers have evaluated the thermodynamic relations in this and other clay systems. Tardy and Garrels (1974), Nriagu (1975), Mattigod and Sposito (1978), Sposito (1986), and Chermak and Rimstidt (1989) used additivity methods to estimate the free energy of various illite, smectite, and other clay mineral samples. Such methods will produce linear G/X relations for solid solutions, implying no free energy of mixing and negative deviations from ideality for a/X relations that are most unlikely. Whereas they may provide first-order estimates of free energies of formation, errors of several tens of kilojoules per mole must be anticipated for additivity approaches, which do not include specific mixing terms for solid solutions. In any case, simple additivity schemes cannot be used to evaluate a/X relations of solid solutions. Stoessell (1979) and Aagaard and Helgeson (1983) applied Temkin-type mixing models that assume independent and ideal mixing of K vs. vacancies and Si vs. Al to illite solutions on the pyrophyllite-muscovite binary. The assumption of ideal mixing on the two sites is unreasonable considering the importance of local charge balance for the detailed understanding of the crystal chemistry of ionic solids. Stoessell (1981) considered quasichemical and electrostatic models for pyrophyllite-muscovite-phlogopite solid solutions at 100°C. Stoessell's model shows negative deviations from ideality between pyrophyllite and muscovite, implying that

the entire solid solution series, including illite, is stable as a result of choosing constants that stablized illite over pyrophyllite + muscovite. Helgeson and Aagaard (1985) remodeled the mixing relations on the pyrophyllite-muscovite binary system with a nonideal mixing model for Al and Si assuming that muscovite has completely disordered $Al^{IV}$ and $Si^{IV}$. They inferred a wide solvus between $Py_{90-94}$ and $Mu_{95.5-96.5}$ at room temperature, but the calculated width of the miscibility gap was clearly model-dependent, and the importance of short-range order in muscovite is yet to be evaluated thermodynamically. The diversity of the results derived from all these models is in part due to the use of arbitrarily selected parameters. Nevertheless, the model and parameters of Helgeson and Aagaard (1985) are consonant with our conclusions as to the intrinsic metastability of illite and the wide miscibility gap between pyrophyllite and muscovite.

### Geological implications

The question of whether or not illite, smectite, and other clay minerals are metastable or stable has important implications for the interpretation of geological systems in which they occur. If they are stable phases at any given pressure, temperature, and bulk composition, they could be utilized as indicators of absolute temperature; i.e., the conversion of smectite to illite or illite to muscovite ("illite crystallinity") would be a valid measure of temperature, and could be used as an unambiguous measure of grade of diagenesis/metamorphism, similar to the plethora of transitions utilized by petrologists in metamorphic rocks corresponding to greenschist facies and higher grade rocks. If, on the other hand, clay minerals are metastable, they owe their occurrences to kinetic factors, only one of which is temperature. Lippmann (1981) emphasized that, in this context, clay mineral diagenesis involves a series of reaction steps, each one of which results in a decrease in free energy, with the clay minerals present at any step being metastable. The stable phases are only attained near greenschist facies conditions. This "Ostwald-step-rule-like" series of transitions ("Ostwald ripening") has been reviewed in the general context of sedimentary diagenesis by Morse and Casey (1988). Because the sequence of transitions in dioctahedral clay minerals from smectite through illite involves a sequence of metastable phases of progressively lower energy, it is a rather typical example of the application of the Ostwald step rule.

The critical point is that the occurrence of any clay mineral must be a measure of "reaction progress" as determined by reaction kinetics, and that any variable affecting reaction rates, among which temperature is only one such variable, can determine the occurrence of a given clay mineral. For example, the role of a fluid phase may be at least as significant as temperature in promoting reactions at low grades (Ahn *et al.,* 1988). Clearly, absolute temperatures cannot be determined

only on the basis of the observed mineralogy in such systems. This is not to say that the phases occurring in such systems will not change in a regular and predictable way with increasing temperature; they will, and do. It only emphasizes that the state of such systems is a measure of "reaction progress," with approximate temperatures being determinable only if the other variables affecting reaction progress are shown to have minimal effects.

## ACKNOWLEDGMENTS

## REFERENCES

Aagaard, P. and Helgeson, H. C. (1983) Activity/composition relations among silicates and aqueous solutions: II. Chemical and thermodynamic consequences of ideal mixing of atoms on homological sites in montmorillonites, illites, and mixed-layer clays: *Clays & Clay Minerals* **31**, 207–217.

Ahn, J. H., Peacor, D. R., and Coombs, D. S. (1988) Formation mechanisms of illite, chlorite and mixed-layer illite-chlorite in Triassic volcanogenic sediments from the Southland Syncline, New Zealand: *Contrib. Mineral. Petrol.* **99**, 82–89.

Ahn, J. H., Peacor, D. R., and Essene, E. J. (1985) Coexisting paragonite-phengite in blueschist eclogite: A TEM study: *Amer. Mineral.* **70**, 1193–1204.

Baldelli, C., Franceschelli, M., Leoni, L., and Memmi, I. (1989) Ferrimuscovite and celadonite substitutions in muscovite from Fe³⁺-rich low-grade psammitic rocks (Northern Apennines, Italy): *Lithos* **23**, 201–208.

Baxter, S. M. and Peacor, D. R. (1988) TEM observation of polytypism in illite: in *Program and Abstracts, 25th Annual Meeting, Grand Rapids, Michigan,* The Clay Minerals Society, p. 74.

Bucher-Nurminen, K. (1987) A recalibration of the chlorite-biotite-muscovite geobarometer: *Contrib. Mineral. Petrol.* **96**, 519–522.

Burst, J. F., Jr. (1959) Post-diagenetic clay mineral environmental relationships in the Gulf Coast Eocene: in *Clays and Clay Minerals, Proc. 6th Natl. Conf., Berkeley, California, 1957,* Ada Swineford, ed., Pergamon Press, New York, 327–341.

Burst, J. F., Jr. (1969) Diagenesis of Gulf Coast clayey sediments and its possible relation to petroleum migration: *Bull. Amer. Assoc. Petrol. Geol.* **53**, 73–93.

Burtner, R. I. and Warner, M. A. (1986) Relationship between illite/smectite diagenesis and hydrocarbon generation in Lower Cretaceous Mowry and Skull Creek shales of the northern Rocky Mountain area: *Clays & Clay Minerals* **34**, 390–402.

Chang, H. K., Mackenzie, F. T., and Schoonmaker, J. (1986) Comparisons between the diagenesis of dioctahedral and trioctahedral smectite, Brazilian offshore basins: *Clays & Clay Minerals* **34**, 407–423.

Chermak, J. A. and Rimstidt, J. D. (1989) Estimating the thermodynamic properties (ΔG°$_f$ and ΔH°$_f$) of silicate minerals at 298 K from the sum of polyhedral contributions: *Amer. Mineral.* **74**, 1023–1031.

Dunoyer de Segonzac, G. (1970) The transformation of clay minerals during diagenesis and low-grade metamorphism: A review: *Sedimentology* **15**, 281–346.

Essene, E. J. (1982) Geologic thermometry and barometry: in *Characterization of Metamorphism Through Mineral Equilibria, Reviews in Mineralogy, Vol. 10,* J. M. Ferry, ed., Mineralogical Society of America, Washington, D.C., 153–206.

Essene, E. J. (1989) The current status of thermobarometry in metamorphic rocks: in *Evolution of Metamorphic Belts,* J. S. Daly, R. A. Cliff, and B. W. D. Yardley, eds., *Geological Society Special Publication 43,* The Geological Society of America, Boulder, Colorado, 1–44.

Foster, M. D. (1956) Correlation of dioctahedral potassium micas on the basis of their charge relations: *U.S. Geol. Surv. Bull.* **1036D**, 57–67.

Franceschelli, M., Mellini, M., Memmi, I. and Ricci, C. A. (1986) Fine-scale chlorite-muscovite association in low-grade metapelites from Nurra (NW Sardinia), and the possible misidentification of metamorphic vermiculite: *Contrib. Mineral. Petrol.* **93**, 137–143.

Franceschelli, M., Mellini, M., Memmi, I., and Ricci, C. A. (1989) Sudoite, a rock-forming mineral in Verrucano of the Northern Apennines (Italy) and the sudoite-chloritoid-pyrophyllite assemblage in prograde metamorphism: *Contrib. Mineral. Petrol.* **101**, 274–279.

Frey, M., Saunders, J., and Schwander, H. (1988) The mineralogy and metamorphic geology of low-grade metasediments, Northern Range, Trinidad: *J. Geol. Soc. London* **145**, 563–575.

Frey, M., Teichmueller, M., Teichmueller, R., Mullis, J., Kunze, B., Breitschmid, A., Gruner, U., and Schwizer, B. (1980) Very low grade metamorphism in external parts of the Central Alps: illite crystallinity, coal rank and fluid inclusion data: *Eclogae Geologicae Helvetiae* **73**, 173–203.

Garrels, R. M. (1984) Montmorillonite/illite stability diagrams: *Clays & Clay Minerals* **32**, 33–48.

Ghent, E. D., Stout, M. Z., and Ferri, F. (1989) Chloritoid-paragonite-pyrophyllite and stilpnomelane-bearing rocks near Blackwater Mountain, western Rocky Mountains, British Columbia: *Canad. Mineral.* **27**, 59–66.

Grim, R. E. (1968) *Clay Mineralogy,* 2nd ed., McGraw-Hill, New York, 31–50.

Helgeson, H. C. and Aagaard, P. (1985) Activity/composition relations among silicates and aqueous solutions: I. Thermodynamics of intrasite mixing and substitutional order/disorder in minerals: *Amer. J. Sci.* **285**, 769–844.

Hoffman, J. and Hower, J. (1979) Clay mineral assemblages as low-grade metamorphic geothermometers: Application to thrust faulted disturbed belt of Montana, USA: in *Aspects of Diagenesis,* P. A. Scholle and P. R. Schluger, eds., *Soc. Econ. Paleontol. Mineral. Spec. Publ.* **26**, 55–79.

Hower, J., Eslinger, E. V., Hower, M. E., and Perry, E. A. (1976) Mechanism of burial metamorphism of argillaceous sediments: 1. Mineralogical and chemical evidence: *Geol. Soc. Amer. Bull.* **87**, 725–737.

Hunziker, J. C., Frey, M., Claver, N., Dollmeyer, R. D., Friedrickson, H., Flehmig, W., Hochstrasser, K., Roggwiler, P., and Schwander, H. (1986) The evolution of illite to muscovite: Mineralogical and isotopic data from the Grlarus Alps, Switzerland: *Cont. Mineral. Petrol.* **92**, 157–180.

Juster, T. C. and Brown, P. E. (1984) Fluids in pelitic rocks during very low-grade metamorphism: *Geol. Soc. Amer. Abstr. Prog.* **16**, p. 553.

Juster, T. C., Brown, P. E., and Bailey, S. W. (1987) NH₄-bearing illite in very low grade metamorphic rocks associated with coal, northeastern Pennsylvania: *Amer. Mineral.* **72**, 555–565.

Kanehira, K. and Banno, S. (1960) Ferriphengite and aegirine-jadeite in a crystalline schist of the Iimori District, Kii Peninsula: *J. Geol. Soc. Japan* **66**, 654–659.

Kisch, H. J. (1983) Mineralogy and petrology of burial diagenesis (burial metamorphism) and incipient metamorphism in clastic rocks: in *Diagenesis in Sediments and Sedimentary Rocks 2,* G. Larsen and G. V. Chilingar, eds., Elsevier, New York, 289–493.

Kisch, H. J. (1987) Correlation between indicators of very low-grade metamorphism: in *Low Temperature Metamorphism,* M. Frey, ed., Chapman and Hall, New York, 227–300.

Kubler, B. (1964) Les argiles, indicateurs de metamorphisme: *Rev. Inst. Franc. Petrol.* **19,** 1093–1112.

Lee, J. H., Peacor, D. R., Lewis, D. D., and Wintsch, R. P. (1986) Evidence for syntectonic crystallization for the mudstone to slate transition at Lehigh Gap, Pennsylvania, U.S.A.: *J. Struct. Geol.* **8,** 767–780.

Lippmann, F. (1981) Stability diagrams involving clay minerals: in *8th Conf. on Clay Mineralogy and Petrology, Teplice 1979,* J. Konta, ed., Univerzita Karlova, Praha, Czechoslovakia, 153–171.

Lippmann, F. (1982) The thermodynamic status of clay minerals: in *Proc. Int. Clay Conf. Bologna, Pavia, 1981,* H. van Olphen and F. Veniale, eds., Elsevier, New York, 475–485.

Massonne, H. J. and Schreyer, W. (1987) Phengite geobarometry based on the limiting assemblage with K-feldspar, phlogopite and quartz: *Contrib. Mineral. Petrol.* **96,** 212–24.

Mattigod, S. V. and Sposito, G. (1978) Improved method for estimating the standard free energies of formation ($\Delta G_{f,298.15}$) of smectites: *Geochim. Cosmochim. Acta* **42,** 1753–1762.

May, H. M., Kinniburgh, D. G., Helmke, P. A., and Jackson, M. L. (1986) Aqueous dissolution, solubilities and thermodynamic stabilities of common aluminosilicate minerals: Kaolinite and smectites: *Geochim. Cosmochim. Acta* **50,** 1667–1677.

Merino, E. and Ransom, B. (1982) Free energies of formation of illite solid solutions and their compositional dependence: *Clay & Clay Minerals* **30,** 29–39.

Morse, J. W. and Casey, W. H. (1988) Ostwald processes and mineral paragenesis in sediments: *Amer. J. Sci.* **288,** 537–560.

Nadeau, P. H. and Reynolds, R. C., Jr. (1981) Burial and contact metamorphism in the Mancos Shale: *Clays & Clay Minerals* **29,** 249–259.

Nriagu, J. O. (1975) Thermodynamical approximations for clay minerals: *Amer. Mineral.* **60,** 834–839.

Phillips, G. N. (1987) Metamorphism of the Witwatersrand gold fields: Conditions during peak metamorphism: *J. Metamorphic Geol.* **5,** 307–322.

Prigogine, I. and Defay, R. (1954) *Chemical Thermodynamics,* translated from the 2nd French ed. by D. H. Everett, Longmans, Green & Co., New York.

Sass, B. M., Rosenberg, P. E., and Kittrick, J. A. (1987) The stability of illite/smectite during diagenesis: An experimental study: *Geochim. Cosmochim. Acta* **51,** 2103–2115.

Sposito, G. (1986) The polymer model of thermodynamical clay mineral stability: *Clays & Clay Minerals* **34,** 198–203.

Środoń, J. and Eberl, D. D. (1984) Illite: in *Micas,* S. W. Bailey, ed., *Reviews in Mineralogy, Vol. 13,* Mineralogical Society of America, Washington, D.C., 495–544.

Środoń, J., Morgan, D. J., Eslinger, E. V., Eberl, D. D., and Karlinger, M. R. (1986) Chemistry of illite/smectite and end member illite: *Clays & Clay Minerals* **34,** 368–378.

Stoessell, R. K. (1979) A regular solution site-mixing model for illite: *Geochim. Cosmochim. Acta* **43,** 1151–1159.

Stoessell, R. K. (1981) Refinements in a site-mixing model for illites: Local electrostatic balance and the quasi-chemical approximation: *Geochim. Cosmochim. Acta* **45,** 1733–1741.

Tardy, Y. and Garrels, R. M. (1974) A method for estimating the Gibbs energies of formation of layer silicates: *Geochim. Cosmochim. Acta* **38,** 1101–1116.

van der Pluijm, B. A., Lee, J. H., and Peacor, D. R. (1988) Analytical electron microscopy and the problem of potassium diffusion: *Clays & Clay Minerals* **36,** 498–504.

Velde, B. (1965) Phengite micas: Synthesis, stability and natural occurrence: *Amer. J. Sci.* **263,** 886–913.

Velde, B. (1969) The compositional join muscovite-pyrophyllite at moderate pressures and temperatures: *Bull. Soc. Fr. Mineral. Cristallogr.* **92,** 360–368 (in French).

Weaver, C. E. (1960) Possible uses of clay minerals in search for oil: *Bull. Amer. Assoc. Petrol. Geol.* **44,** 1505–1518.

Yau, Y. C., Peacor, D. R., Essene, E. J., Lee, J. H., Kuo, L. C., and Cosca, M. A. (1987) Hydrothermal treatments of smectite, illite, and basalt to 460°C: Composition of natural with hydrothermally formed clay minerals: *Clays & Clay Minerals* **35,** 241–250.